Analysis of non-derivatised bacteriohopanepolyols by ultrahigh performance liquid chromatography-tandem mass spectrometry

Helen M. Talbot[1]*, Frances R. Sidgwick[1,2], Juliane Bischoff[1], Kate A. Osborne[1], Darci Rush[1], Angela Sherry[1], Charlotte L. Spencer-Jones[1***]**

[1]School of Civil Engineering and Geosciences, Newcastle University, Newcastle upon Tyne, NE1 7RU, UK

[2]Newcastle University Protein and Proteome Analysis (NUPPA), Devonshire Building, Newcastle University, Newcastle upon Tyne, NE1 7RU, UK

Correspondence to. H. M. Talbot, School of Civil Engineering and Geosciences, Drummond Building, Newcastle University, Newcastle upon Tyne, NE1 7RU, UK

E-mail: helen.talbot@ncl.ac.uk

** *Now at:* The Lyell Centre, Heriot-Watt University, Edinburgh, UK

*** *Now at:* Department of Geography, University of Durham, Durham, UK

RATIONALE: Traditional investigation of bacteriohopanepolyols (BHPs) has relied on derivatisation by acetylation prior to gas chromatography-mass spectrometry (GC/MS) or liquid chromatography-MS (LC/MS) analysis. Here, modern chromatographic techniques (ultrahigh performance liquid chromatorgraphy) and new column chemistries were tested to develop a method for BHP analysis without the need for derivatisation.

METHODS: Bacterial culture and sedimentary lipid extracts were analysed using a Waters Acquity Xevo TQ-S in positive ion atmospheric pressure chemical ionisation (APCI) mode. Waters BEH C18 and ACE Excel C18 were the central columns evaluated using a binary solvent gradient with 0.1% formic acid in the polar solvent phase in order to optimise performance and selectivity.

RESULTS: Non-amine BHPs and adenosylhopane showed similar performance on each C18 column, however, BHPs containing terminal amines were only identified eluting from the ultra-inert ACE Excel C18 column. APCI MS-MS product ion scans revealed significant differences in fragmentation pathways compared to previous methods for acetylated compounds. Fragment ions for targeted multiple reaction monitoring (MRM) are summarised.

CONCLUSIONS: UPLC/MS-MS analysis using an ACE Excel C18 column produced superior separation for amine-containing BHPs and reduced run times from 60 to 9 min compared to previous methods. Unexpected variations in fragmentation pathways between structural subgroups must be taken into account when optimising MRM transitions for future quantitative studies.

Bacteriohopanepolyols (BHPs) are microbial membrane lipids occurring ubiquitously in the environment although they are estimated to be produced by less than 10% of bacteria (see Fig. 1 for examples).[1,2] They can be used as biomarkers to indicate specific bacterial populations and/or processes such as aerobic methane oxidation[3-5] or the transport of soil organic matter via rivers or coastal erosion to the marine environment.[6-10] They are also the biological precursors of the geohopanoids (hopanols, hopanoic acids, hopanes) which have been described as the most abundant natural products on earth.[11]

Analytical methods for identification and (semi) quantification of complex mixtures of the BHPs have typically utilised acetylation of the functional amine and hydroxyl groups, followed by either gas chromatography mass spectrometry (GC/MS) which can only detect a limited number of compounds[12] or reversed phase high performance liquid chromatography (HPLC) with ion-trap multiple stage mass spectrometry (MS^n) detection.[13-18] The first HPLC method for BHP separation without prior derivatisation involved a simple normal phase HPLC system with a silica 60 column and ternary solvent gradient of *n*-hexane, propan-2-ol and 0.04% triethylamine in water.[19] This system was able to separate 3 common BHPs: bacteriohopane-32,33,34,35-tetrol (BHT herein; **Ia**, Fig. 1), BHT-glucosamine (**Ib**) and BHT-cyclitol ether (**Ic**). This separation method was later adapted and, when coupled to mass spectrometer using negative ion chlorine addition under atmospheric pressure chemical ionisation (APCI) conditions, was able to identify these compounds in lake sediments.[20] However, subsequent investigation of this method revealed that it was unsuitable for other commonly occurring BHPs with a terminal amine moiety at the C-35 position (such as 35-aminobacteriohopane-32,33,34-triol [aminotriol herein]; **Id**, Fig. 1) as they were strongly retained resulting in extended analysis times and poor peak shapes.[13] Subsequently analyses by LC/MS were undertaken on peracetlyated samples using reversed phase chromatography with either a ternary or binary solvent system changing linearly from methanol (MeOH):water (90:10) to propan-2-ol:MeOH:water (40:59:1) and with detection via positive ion APCI.[13,15,16,21,22]

More recently, Malott et al.[23] reported the identification of non-derivatised BHPs using an ultra-performance liquid chromatography-mass spectrometry (UPLC/MS) method based on a Waters (Inc.) application note for lipid analysis.[24] Briefly, samples were separated using a charged surface hybrid (CSH) C_{18} column (Waters Acquity UPLC CSH C_{18}, 2.1 x 100 mm, 1.7 μm) with a binary solvent system containing 10 mM ammonium formate and 0.1% formic acid eluted at 0.4 mL/min with the column maintained at 55°C. Analysis was via Waters LC-tandem MS (LC-

MS/MS) system (Acquity I class UPLC with a Xevo G2-S time of flight (TOF) mass spectrometer). Column eluent was ionized by electrospray ionization in both positive and negative-ion mode. However, only BHT cyclitol ether (**Ic**), the dominant hopanoid from *Burkholderia multivorans*, was reported including the protonated (*m/z* 708.5451) and sodiated form (*m/z* 730.5225). Identification of this structure is in agreement with previous studies of *Burkholderia* spp..[25] However, unsaturated BHT-CE (**Ic** with double bond at C-6) as well as BHT (**Ia**) which have also been detected from this genus were not reported.[17,25] The same UPLC/MS-MS method was also employed by Wu et al.[26] to identify BHT and 2Me-BHT (**IIa**). These authors also reported significantly reduced ionisation efficiencies for non-acetylated compounds relative to the equivalent mass of the acetylated structures. This was proposed as potentially resulting from the low solubility of these compounds in the solvent used for LC/MS (dilution via sonication in propan-2-ol:acetonitrile:water; 2:1:1).

Further development of an UPLC/MS method for the identification and ultimately the quantification of a much wider range of BHP compounds will therefore be beneficial to significantly reduce the use of solvents and chemicals such as acetic anhydride and pyridine, which are currently widely employed for derivatisation, whilst increasing separation potential and/or sensitivity and sample throughput by reducing analysis time (currently 60 min per sample, HPLC method using reversed phase C_{18} HPLC separation.[17,18] Here, we report on the first stage of development of a new UPLC/MS-MS method considering a range of columns (including different manufacturers and different phases for enhanced selectivity) and also assess fragmentation patterns to establish optimal precursor-product ion transitions, often with unexpected difference to previously reported hopanoid mass spectra.

EXPERIMENTAL

Materials

Bacterial cultures of *Methylosinus trichosporium* OB3b and *Methylococcus capsulatus* Bath as well as River Tyne (UK) estuary surface sediment were available in house.[27, 28] All samples were freeze dried, ground to a fine powder then extracted (~20 mg for cell mass and ~1 g for sediment) as described previously using a modified Bligh and Dyer method to produce a total lipid extract (TLE; for full details see[29,30]).

Solid phase extraction

Further clean-up of the TLE is required prior to UPLC/MS-MS analysis therefore aliquots of TLE were pre-treated with aminopropyl solid phase extraction (SPE) to produce a concentrated polar-fraction containing all BHPs. The SPE method used was adapted from a method commonly applied in other studies of complex polar lipids from environmental samples which produces a neutral (chloroform:propan-2-ol; 2:1), acid (2% acetic acid in diethylether) and polar (MeOH) fraction.[31] However, preliminary analysis revealed that although the majority of the BHPs were eluted as expected in the polar fraction, some BHPs such as adenosylhopane (**Ie**) and related compounds (**IIe**, **If**, **IIf**, **If'**, **IIf'**) were at least partially recovered in the neutral fraction. Therefore, the method was further adapted as follows. Isolute (Biotage, Uppsala, Sweden) NH_2 1 g/6 mL SPE columns were preconditioned with 2 x 3 mL hexane. Sample TLE was reconstituted in chloroform (200 μL) and loaded onto the column. Fraction 1 (non-polar+acids) was eluted with acetic acid/diethylether (2:98 v/v, 6 mL). Fraction 2 (Polar fraction) was eluted with MeOH (10 mL). All fractions were blown down to dryness under N_2. Fraction 1 (non-polar+acids) was not investigated further as it does not contain BHPs. It was also noted that the 5α-pregnane-3β,20β-diol standard which is typically added to the TLE prior to further treatment or analysis (e.g.[32]) elutes in the non-polar fraction if added to the TLE prior to SPE.

Derivatisation and filtering

For comparison of derivatised and non-derivatised polar fractions, aliquots of the polar fractions were evaporated to dryness under N_2 and acetylated by adding acetic anhydride and pyridine (0.25 mL each), heated at 50°C for 1 h then left at room temperature overnight to yield acetylated BHPs. The acetic anhydride and pyridine was removed under a stream of N_2 and the resulting acetylated sample was dissolved in 1 mL MeOH/propan-2-ol (3:2, v/v). All fractions, derivatised and non-derivatised, were filtered through 0.22 μm PTFE filters (VWR International Ltd., Lutterworth, Leicestershire, UK) prior to analysis by UPLC/MS-MS.

UPLC/MS-MS analysis of non-derivatised BHPs

Separation of the polar fraction BHPs was performed on a Waters (Elstree, UK) Acquity UPLC system fitted with either a Waters Acquity UPLC BEH C18 column (1.7 μm, 2.1 mm x 100 mm; PN: 186002352) and an Acquity BEH C18 VanGuard pre-column (all supplied by Waters, UK) . or an ACE Excel UHPLC C18 column (2 μm, 2.1 mm x 100 mm; PN: EXL-101-1002U) fitted with an ACE Excel UHPLC Pre-column filter (PN: EXL-PCF10; all ACE columns supplied by

Hichrom Ltd., Reading, UK). Additional ACE excel phases (AR, Amide, PFP and Super C18) were tested for alternative selectivity using identical column dimensions and particle size to the C18 column. All showed reduced chromatographic performance relative to the C18 for non-derivatised BHPs although the AR column did show slightly improved separation of methylated compounds related to adenosylhopane. The solvent gradient was based on that used previously for derivatised BHPs under HPLC conditions which comprises 90% MeOH, 10% Water at Time 0 followed by a liner gradient to 59% propan-2-ol, 40% MeOH, 1 % water in 25 min.[17,18] For UPLC of non-derivatised compounds the more polar solvent phase was modified with 0.1% formic acid (99% ULC/MS grade; Biosolve [Dieuze, France], supplied by Greyhound Chromatography and Allied Chemicals, Birkenhead, UK). The following profile, adapted from that used for HPLC-MS analysis, was found to provide the best compromise between separation of compounds, peak shape and run time: 100% A (Time 0) to 100% B (at 3.5 min), isocratic for 2 min then returning to the starting conditions in 0.5 min and stabilising for 3 min before the next injection (solvent mix A = MeOH:water:formic acid [90:10:0.1 v/v/v] and B = propan-2-ol:MeOH:water [59:40:1 v/v/v]. All solvents were Biosolve ULC/MS grade (supplied by Greyhound Chromatography and Allied Chemicals). The flow rate for all runs was 0.6 mL/min and the column was heated to 40°C. Samples (i.e. one half of the SPE polar fractions) were dissolved in MeOH:propan-2-ol (3:2 v/v) and injected via an Acquity Sample Manager fitted with a 30 μL all PEEK sample needle (Waters Ltd., Elstree, UK; PN: 700002644). Use of the PEEK needle was required to eliminate contamination of samples, as initial tests showed pronounced carryover for the non-derivatised primary amines, particularly 35-aminobacteriohopane-32,33,34-triol (**Id**), when using the standard (stainless steel) needle.

Detection was carried out with a Waters Xevo TQ-S (triple quadrupole with StepWave - a unique, patented off-axis ion transfer device which maximises sensitivity by actively removing neutrals to reduce contamination), operated in positive ion mode fitted with a combined atmospheric pressure (chemical) ionisation and atmospheric pressure photoionisation (API-APPI) source, but operated in API only mode. Tuning and optimisation of parameters was achieved using a standard solution of 5α-pregnane-3β,20β-diol. Conditions were as follows: corona discharge 0.3 μA, cone voltage 30 V, source offset 50 V, gas flow rates (N_2): Desolvation 250 L h^{-1}, Cone 150 L h^{-1}. The nebuliser pressure was set to 4 Bar.

Preliminary determination of parent-product ion transitions for BHT (**Ia**; parent ion *m/z* 529 = $[M+H-H_2O]^+$) and aminotriol (**Id**; parent ion *m/z* 546 = $[M+H]^+$) was achieved via off-column

loop-injections of aliquots of TLE of *M. trichosporium*.[33] Product ion spectra were obtained at a range of collision energies from 20 to 35 eV. Product ion spectra of other compounds were obtained on-line during chromatographic runs of River Tyne sediment SPE polar fraction. Subsequently, typical values used for multiple reaction monitoring (MRM) transitions were cone voltage 30 eV and collision energy 30 eV unless otherwise stated below.

To assess if observed difference in BHP spectra were due to acetylation (or absence of acetylation) or were due to the differences in instrumentation (ion-trap vs. quadrupole MS-MS) we also obtained comparable product ion scans of acetylated BHPs using the UPLC/MS-MS. The system was set up as described above except without the formic acid solvent modifier in solvent A. The analytical conditions used for analysis of derivatised BHPs by HPLC-ion-trap-MS^n on a Thermo Finnigan Surveyor-LCQ system have been described in detail elsewhere.[17,18,29,32]

RESULTS AND DISCUSSION

Bacteriohopane-32,33,34,35-tetrol (BHT)

Bacteriohopanetetrol (BHT; **Ia**) is the most commonly occurring of all known BHP structures and has been reported widely in bacterial cultures and modern, recent and ancient samples up to 56 Ma.[3,34-36] The acetylated BHT protonated molecule ($[M+H]^+$ = *m/z* 715) is unstable under APCI conditions, resulting in rapid loss of one functional group and a base peak ion of *m/z* 655 ($[M+H-CH_3COOH]^+$). This loss of one functional group to form the base peak ion is seen for all acetylated BHPs that do not contain N unless they contain a heterocyclic O atom resulting in a base peak ion of $[M+H]^+$.[37] The ion-trap MS^2 spectrum of BHT (from parent ion *m/z* 655; Fig. 2a), which has been described in detail elsewhere,[15,16] contains ions indicating loss of the functional groups (as CH_3COOH, -60 Da) and ions indicating loss of the A+B ring fragment including an ion of *m/z* 191 (Fig. 2a). Under electron impact ionisation the *m/z* 191 ion is the major ion fragment observed indicating ring system cleavage of the C8 –C14 bond and the C-9 to C-11 bond.[38] This ion or the equivalent *m/z* 205 ion in hopanoids methylated on the A-ring (e.g. **IIa**, **IIIa**) are used as characteristic ions during selected ion monitoring of hopanoids during GC/MS analysis.[12] After confirming the presence of BHT in the SPE polar fraction of River Tyne estuary sediment extract via acetylation of a portion of the SPE polar fraction and analysis via the standard HPLC-MS^n method, [15-18] product ion scans were also obtained for the acetylated compound under UPLC/MS-MS (examples shown at 30 eV collision energy; Fig. 2b). Although ions indicative of the full (-

60 Da) or partial loss of the acetylated functional groups (as CH_2CO, 42 Da) were common to both ion-trap and triple quadrupole spectra of the acetylated parent ion (*m/z* 655; Fig. 2a and b, respectively), the lower mass range of the quadrupole spectrum was different to that expected via comparison of the EI –MS spectrum of BHT.[38]. Ions of *m/z* 369 (indicating charge retention on the ring system after loss of the side chain) and *m/z* 191 (A+B rings) were present but relatively minor compare to lower mass ions (Fig. 2b).

To obtain product ion scans from the parent ion *m/z* 529 (= $[M+H-H_2O]^+$)of non-acetylated BHT (**Ia**) (Table 1), loop injection of TLE from the methanotrophic bacterium *Methylosinus trichosporium* OB3b, which is known to contain BHT,[33] were performed with product ion scans recorded at a range of collision energies (CE). At 20 eV CE fragmentation was limited and the base peak ion was still *m/z* 529 (Fig. 2c). Other ions included *m/z* 511 (loss on one additional OH group as H_2O), *m/z* 369 and *m/z* 191. However, the major fragment in the lower mass range was *m/z* 163 (Fig. 2c); also present and more intense than *m/z* 191 in the spectrum of the acetylated compound under identical conditions (Fig. 2b). The exact structure of this ion is unknown, however an ion of the same *m/z* value has been observed previously in the APCI-MS^2 spectrum of acetylated BHT and other related compounds.[15] and was more intense than the *m/z* 191 ion at all collision energies (e.g. Fig. 2c,d). With increasing collision energy (30 eV, Fig. 2d), the ions *m/z* 511, 369 and 191 were still present but at even lower relative intensity and low *m/z* value fragment ions assumed to derive from the ring system dominate the spectrum. At 30 eV the base peak ion in the product ion scan is *m/z* 95 with *m/z* 163 approximately 80% of the intensity of the base peak (Fig. 2d). Given the low intensity of the *m/z* 191 ion which would be the expected choice for an MRM ion transition (*m/z* 529 to *m/z* 191) by comparison with EI spectra, we instead suggest that the ion transition *m/z* 529 to *m/z* 163 could provide a more intense signal for detection and quantification. Proposed target ion transitions for other common BHPs containing no N atoms are indicated in Table 1 (**IIa**, **Ig**, **Ih**).

35-Aminobacteriohopane-32,33,34-triol (aminotriol)

The tetrafunctionalised 35-amino-bacteriohopane-32,33,34-triol (**Id**) is the second most commonly reported BHP, found in a wide range of cultured organisms and environments.[3,30,39] When acetylated, the parent ion is *m/z* 714 $[M+H]^+$ and when not acetylated, *m/z* 546 (Table 1). We have previously proposed that the stability of the protonated acetylated amine limits fragmentation under APCI MS^n analysis to simple side chain fragmentation i.e. loss of acetylated hydroxyls (Fig. 3a). The APCI-MS-MS product ion spectrum of the acetylated compound (from

parent ion *m/z* 714) at 30 eV CE (Fig. 3b) is also dominated by fragments from the side chain but does contain minor ions at *m/z* 191 and 163, though much less intense than those seen in the equivalent spectrum of BHT (Figs. 2b and 3b). As for BHT, loop injections of TLE from *M. trichosporium* were performed to obtain product ion spectra of the non-acetylated aminotriol (from parent ion *m/z* 546; **Id**). At 20 eV collision energy only limited fragmentation is observed with one minor ion of *m/z* 528 (loss of OH as H_2O; Fig. 3c). However, at 35 eV CE, (Fig. 3d) more significant fragmentation is observed with a base peak of *m/z* 95 (as seen for BHT at 30 eV CE (Fig. 2d). The next most intense ion is *m/z* 528 which is accompanied by ions *m/z* 510 and 492 indicating loss of a second and third OH, respectively. Loss of the amine is not observed, similar to the ion-trap MS^2 spectrum (Fig. 3a). Again *m/z* 163 is observed and is more abundant than *m/z* 191 with both of these ions less than 50% intensity of the *m/z* 528 ion. We therefore propose that the MRM transition from the parent ion *m/z* 546 to *m/z* 528 is the best target for aminotriol. However, as loss of water is not highly specific, additional target ions of either *m/z* 191 or *m/z* 163 (Fig. 3d) should also be employed to support the assignment. More generally for any C-35 amine-containing BHP that the generic transition $[M+H]^+$ to $[M+H-H_2O]^+$ together with a more diagnostic ring-system ion (*m/z* 191 or 163 – or equivalent for methylated compounds) should be the target MRMs for these important compounds. The relevant ions for targeted MRM scans for the most commonly occurring structures of this group, including C-3 methylated compounds, are indicated in Table 1 (**Id**, **IId**, **IIId**, **Ii**, **IIIi**, **Ij**, **IIIj**).

Bacteriohopanetetrol cyclitol ether (BHT-CE)

Bacteriohopanetetrol cyclitol ether (BHT-CE; **Ic**) is the most commonly occurring of a group of compounds termed "composite BHPs" i.e. BHPs with a regular, linear side chain (as in BHT or aminotriol, above) but with a more complex functional group such as an amino sugar attached via an ether bond at the C-35 position. When acetylated, the major protonated molecule $[M+H]^+$ is an ion of *m/z* 1002 (heptaacetate form),[15] with a subordinate contribution from the octaactetate ($[M+H]^+$ = *m/z* 1044).[16] The ion-trap MS^2 spectra and MS-MS product ion scans of the heptaacetate are similar (Fig. 4a and b, respectively), with major fragments arising from loss of one or more acetylated hydroxyls (*m/z* 942, 882, 822) or loss of the entire terminal group *m/z* 655 (and *m/z* 595, 535 and 475) after loss of the functional groups at C-32, 33 and 34. Finally, both spectra contain minor ions indicating the terminal moiety of *m/z* 330 and 348 (Fig. 4a,b).

When not acetylated, the protonated molecule $[M+H]^+$ is *m/z* 708 (Table 1). At 20 eV collision energy, the product ion scan only contains one significant fragment ion at *m/z* 162 (Fig. 4c). This

ion fragment is the terminal group (corresponding to *m/z* 330 in the heptaacetate; Fig. 4a,b). At higher collision energy the relative intensity of the *m/z* 162 ion increased and an ion of *m/z* 180 was also observed (Fig. 4d), corresponding to the ion *m/z* 348 in the heptaacetate (Fig. 4a,b). The structure of the ion *m/z* 222 is unknown (Fig. 4d). As the ions *m/z* 162 and 180 will be present in the spectra of all compounds of this type (from parent ion $[M+H]^+$), either with methylation in the ring system or with additional hydroxyls at C-31 (e.g. **Ik**) or C30 and C31 (**Im**), these ions are good targets for MRM transitions as indicated in Table 1.

30-(5'-Adenosyl)hopane (adenosylhopane)

Adenosylhopane (**Ie**) is an important BHP as it is a biosynthetic intermediate in the addition of the side chain to the precursor C_{30} hopanoid diploptene.[40] Unlike the structures described above, the side chain in adenosylhopane is cyclised containing a heterocyclic oxygen atom. When acetylated this structure has been found to produce both di, tri and even tetra acetate (adduct) forms,[29] with protonated molecules of *m/z* 746, 788 and 830, respectively (Table 1). Examples of the mass spectra of the triacetylated form (from parent ion *m/z* 788) from ion-trap (see also[17,29]) and quadrupole MS-MS product ion scan are shown (Fig. 5a,b). In both cases the fragment ion *m/z* 611 $[M+H\text{-adenine}]^+$ dominates the spectrum followed by *m/z* 178 which represents the acetylated adenine moiety.

The non-acetylated protonated molecule $[M+H]^+$ is *m/z* 662 (Table 1). Only one peak was detected in the *m/z* 662 mass chromatogram of the Tyne sediment SPE polar fraction. APCI product ion scans of ion *m/z* 662 at 20 eV was surprisingly simple with the only ions observed being *m/z* 662 and 136 (Fig. 5c; similar to that of BHT-CE at 20 eV collision energy; Fig. 4c). The ion *m/z* 136 is consistent with the protonated adenine moiety after cleavage between of the C-35 to N bond. Increasing the collision energy to 35 eV only increased the intensity of the *m/z* 136 ion and reduced the *m/z* 662 ion; (Fig. 5d) no other fragments were observed even at 40 eV. This observation was unexpected given the more complex spectra of the acetylated compounds from either instrument (Fig. 5a,b).[17] and may be due to stability of the protonated aromatic adenine moiety upon cleavage of the C-N bond. The dominance of a single fragment ion in the product ion spectrum of adenosylhopane (Fig. 5c,d) will produce a strong response during MRM analysis, potentially much higher than for other BHPs which produce multiple ion fragments.

A methylated homologue of adenosylhopane is known (**IIe**,[17] with $[M+H]^+$ 14 Da higher at *m/z* 676 but with the same terminal group (adenine; Table 1). Two other related pairs of methylated and non-methylated homologues are known with each pair comprising a different terminal group (TG; **f** and **f'**) at the C-35 position.[29,41] APCI/MS^n analysis has indicated that the equivalent TG ion to *m/z* 136 in diacetyl-adenosylhopane or *m/z* 178 in triacetyl-adenosylhopane (Fig. 4a,b) for these compounds are *m/z* 151 (from parent ion *m/z* 761, terminal group not acetylated) and *m/z* 192 (from parent ion m/z 802, terminal group with 1 acetylated functionality), respectively. The exact TG structure of these compounds is currently unknown meaning that they are known simply as "Adenosylhopane Type-2" (**If**, **IIf**) and "Adenosylhopane Type-3" (**If'**, **IIf'**), respectively.[6,7] The equivalent $[M+H]^+$ ions for the non-acetylated structures as well as the proposed terminal group ions (by analogy with adenosylhopane; Fig. 4c,d) to be targeted in MRM are indicated in Table 1.

Optimisation of chromatography for non-acetylated BHPs

Having identified suitable target ions for MRM transitions for non-acetylated BHPs (Table 1), a comparison of 2 commonly used UPLC C18 columns was undertaken. The columns chosen were the Waters BEH C18 (1.7 μm particle size, 2.1 x 100 mm) and the ACE Excel C18 (2.0 μm particle size, 2.1 x 100 mm). The latter was chosen as this column is highly base deactivated to facilitate analysis of compounds containing primary amines (e.g. aminotriol, **Id**). Conversion of the standard 60 min gradient used for HPLC analysis of acetylated BHPs on the Phenomenex Gemini C18 (5μ, 3 x 150 mm; 0.5 mL/min)[17,18] to the UPLC columns suggests a linear gradient of 100% solvent mix A (see Methods) to 100% solvent mix B in 3.47 min which we adjusted to 3.5 min. A subsequent isocratic period at 100% B of 2 min duration proved sufficient to allow elution of all commonly occurring BHPs discussed above. The ACE Excel column showed good separation of all major BHPs discussed above in the SPE polar fraction of Tyne River sediment including major (**IIa**) and minor (**IIIa**) methylated isomers of BHT (from parent ion m/z 529 and 543; Fig. 6a). However, we have yet to investigate samples containing other minor isomers or unsaturated structures.[18] Using the same sample, and running under identical chromatographic conditions and detection parameters, but with the Waters BEH C18 column (Fig. 6b) it was possible to detect BHT, both methylated homologues, a related composite BHP similar to BHT-CE but without any N atoms in the structure (BHT-pseudopentose; parent ion *m/z* 691, **In**) and adenosylhopane (parent ion *m/z* 662, **Ie**) with near identical chromatographic separation to the ACE column (except for

partial co-elution of the C-2 and C-3 methylated isomers of BHT; Fig. 6a,b). However, we were unable to detect either the C-35 amines (aminotriol [**Id**], aminopentol [**Ij**]; parent ions m/z 546 and 578 respectively; Fig. 6b) or the amine-containing composite structure BHT-CE (**Ic**; parent ion *m/z* 708) via the Waters BEH C18 column (Fig. 6b), attesting to the excellent base-deactivated properties of the ACE column.

Previously, the full suite of adenosylhopane and related compounds have been observed in River Tyne SPE polar fractions,[27] including adenosylhopane (**Ie**), Type -2 (**If**) and Type-3 (**If'**) and their C-2 methylated homologues (**IIe**, **IIf**, **IIf'**), although the adenosylhopane Type-3 compounds were present only at very low levels (**If'**, **IIf'**; Fig. 7a). Here, using UPLC/MS-MS and selecting MRMs based on the product ion scan of adenosylhopane at 30 V collision energy (Fig. 5d), we were able to also detect the adenosylhopane Type-2 and Type-3 compounds as one strong peak in each MRM trace (*m/z* 677 to *m/z* 151 and *m/z* 676 to *m/z* 150 respectively; Fig. 7b). However, the MRMs for the methylated structures (*m/z* 676 to *m/z* 136, *m/z* 691 to 151 and *m/z* 690 to 150, respectively; Fig. 7b), each showed a cluster of closely eluting peaks. In all cases the major peak (indicated as the **II** homologue in Fig. 7b) co-eluted with the non-methylated compound. The assignment of this peak as the C-2 methylated isomer is based on comparison of the relative position of BHT (**Ia**) and the major methylated homologue (**IIa**) in the River Tyne sediment (Fig. 6a) together with prior knowledge that the C-2 isomer is significantly more abundant in this setting than the C-3 isomer based on multiple analyses of samples taken from the same location using the HPLC-MS^n method for acetylated BHPs.[27] A number of possibilities are considered for the identities of the other peaks. This could include C-3 methylated structures which elute later then the C-2 compounds under these conditions, confirmed via analysis of the SPE polar fraction of a sample of *Methylococcus capsulatus* Bath which is known to biosynthesise C-3 homologues of the primary amines compounds (Fig. 8).[42] Another possibility is a structure related to the novel side-chain methylated compounds recently identified in extracts from the Eocene Cobham Lignite.[36] Although the exact position of the side chain methylation could not be determined in that study, it was proposed that it is most likely to be located at C-31 by comparison with other studies.[43,44] The observation of so many peaks in the putative methylated-adenosylhopanes chromatograms is, however, unexpected as this had not been identifiable in previous analyses via HPLC/MS^n.[29,41]

Towards quantitative analysis

This work has shown that different BHP structures demonstrate very different fragmentation behaviour when acetylated versus not acetylated. This was particularly evident for non-acetylated adenosylhopane which produce only one fragment ion in the MS-MS product ion scan (Fig. 5c,d) promising superior sensitivity to other BHPs which produce multiple fragments under identical conditions and collision energies (Figs. 2, 3, 4). Until such time as authentic standards are available for a wide range of non-acetylated BHP structures, it will not be possible to fully test the sensitivity of the system for quantitative analysis, although we believe this configuration has some advantages over the Malott et al.[23] method. For example, the use of APCI avoids production of sodium adducts and clearly the choice of column is also very important when dealing with compounds containing amines. Other authors reported problems with the dissolution of BHPs in the injection solvent used in their studies. Here, we found that this problem was most significant for the C-35 amine-containing BHPs which also caused problems by contaminating the injection system leading to carry over from one run to the next; however, use of the all PEEK injection needle appears to have resolved this issue. The recently published method for large scale biosynthesis and purification of BHT (**Ia)** and 2-methyl-BHT (**IIa**)[26] is an excellent step towards full quantification, although representative standards of non-derivatised compounds from a range of structural subgroups are still lacking at this time.

CONCLUSIONS

In this study, we have developed a new reversed phase UPLC/MS-MS based method using an ultra inert, base deactivated ACE Excel UHPLC column for the identification of BHPs in lipid extract from an estuary sediment and bacterial cultures, but which can also be applied to lipid extracts from other matrices. MS-MS product ion spectra of non-derivatised BHPs are significantly different to ion trap MS^2 spectra of the equivalent peracetates. Optimising transitions for MRM detection for maximum selectivity shows that sensitivity for adenosylhopane (and related compounds) is significantly enhanced relative to other BHPs and relative to previous methods due to the dominance of a single fragment ion in the APCI spectrum. Separation of some methylated homologues can be enhanced using ACE Excel AR column, although, it has a deleterious effect on the peak shape of other compounds. Authentic non-derivatised pure standards are now required to optimise sensitivity and for quantitative analysis.

Acknowledgements

This work was funded by a Starting Grant (No. 258734) awarded to HMT for project AMOPROX from the European Research Council (ERC). We also thank the Science Research Investment Fund (SRIF) from HEFCE for funding the purchase of the ThermoFinnigan LCQ ion trap mass spectrometer.

REFERENCES

[1] A. Pearson, S. R. F. Page, T. L. Jorgenson, W. W. Fischer, M. B. Higgins. Novel hopanoid cyclases from the environment. *Env. Microbiol.* **2007,** *9*, 2175.

[2] A, Pearson, D. B. Rusch. Distribution of microbial terpenoid lipid cyclases in the global ocean metagenome. *The ISME J.* **2009,** *3*, 352.

[3] H. M. Talbot, R. E. Summons, L.L. Jahnke, C. S. Cockell, M. Rohmer, P. Farrimond. Cyanobacterial bacteriohopanepolyol signatures from cultures and natural environmental settings. *Org. Geochem.* **2008,** *39*, 232.

[4] H. M. Talbot, L. Handley, C. L. Spencer-Jones, B. J. Dinga, E. Schefuß, P. J. Mann, J. R. Poulsen, R. G. M. Spencer, J. N. Wabakanghanzi, T. Wagner. Variability in aerobic methane oxidation over the past 1.2 Myrs recorded in microbial biomarker signatures from Congo fan sediments. *Geochim. Cosmochim. Acta* **2014,** *133*, 387.

[5] C. Berndmeyer, V. Thiel, O. Schmale, M. Blumenberg. Biomarkers for aerobic methanotrophy in the water column of the stratified Gotland Deep (Baltic Sea). *Org. Geochem.* **2013,** *55*, 103.

[6] C. Zhu, H. M. Talbot, T. Wagner, J.-M. Pan, R. D. Pancost. Distribution of hopanoids along a land to sea transect: implications for microbial ecology and the use of hopanoids in environmental studies. *Limnol. Oceanogr.* **2011,** *56*, 1850.

[7] A. Doğrul Selver, H. M. Talbot, Ö. Gustafsson, S. Boult, B. E. van Dongen. Soil organic matter transport along a sub-Arctic river-sea transect. *Org. Geochem.* **2012,** *51*, 63.

[8] A. Doğrul Selver, R. B. Sparkes, J. Bischoff, H. M. Talbot, Ö. Gustafson, I. P. Semiletov, O. V. Dudarev, S. Boult, B. E. van Dongen. Distributions of bacterial and archaeal membrane lipids in surface sediments reflect differences in input and loss of terrestrial organic carbon along a cross-shelf Arctic transect. *Org. Geochem.* **2015,** *83-84,* 16.

[9] J. Bischoff, R. B. Sparkes, A. Doğrul Selver, R. G. M. Spencer, Ö. Gustafson, I. P. Semiletov, O. V. Dudarev, D. Wagner, E. Rivkina, B. E. van Dongen, H. M. Talbot. Source, transport and fate of soil organic matter inferred from microbial biomarker lipids in the East Siberian Arctic Shelf. *Biogeosciences Discussions* **2016,** doi:10.5194/bg-2016-128, 2016

[10] C. J. De Jonge, H. M. Talbot, J. Bischoff, A. Stadnitskaia, G. Charkashov, J. S. Sinninghe Damsté. Bacteriohopanepolyol distribution in Yenisei River and Kara Sea suspended particulate matter and sediments traces terrigenous organic matter input. *Geochim. Cosmochim. Acta* **2016,** *174,* 85.

[11] G. Ourisson, P. Albrecht. Hopanoids. 1. Geohopanoids: the most abundant natural products on Earth? *Acc. Chem. Res.* **1992,** *25,* 398.

[12] A. L. Sessions, L. Zhang, P. V. Welander, D. Doughty, R. E. Summons, D. K. Newman. Identification and quantification of polyfunctionalized hopanoids by high temperature gas chromatography–mass spectrometry. *Org. Geochem*. **2013,** *56,* 120.

[13] H. M. Talbot, D. F. Watson, J. C. Murrell, J. F. Carter, P. Farrimond. Analysis of intact bacteriohopanepolyols from methanotrophic bacteria by reversed phase high performance liquid chromatography - atmospheric pressure chemical ionisation - mass spectrometry. *J. Chrom. A* **2001,** *921,* 175.

[14] H. M. Talbot, D. F. Watson, E. J. Pearson, P. Farrimond. Diverse hopanoid compositions in non-marine sediments. *Org. Geochem.* **2003,** *34,* 1353.

[15] H. M. Talbot, A. H. Squier, B. J. Keely, P. Farrimond. Atmospheric pressure chemical ionisation reversed-phase liquid chromatography/ion trap mass spectrometry of intact bacteriohopanepolyols. *Rapid Commun. Mass Spectrom.* **2003,** *17,* 728.

[16] H. M. Talbot, R. Summons, L. Jahnke, P. Farrimond. Characteristic fragmentation of bacteriohopanepolyols during atmospheric pressure chemical ionisation liquid

chromatography/ion trap mass spectrometry. *Rapid Commun. Mass Spectrom.* **2003,** *17,* 2788.

[17] H. M. Talbot, M. Rohmer, P. Farrimond. Rapid structural elucidation of composite bacterial hopanoids by atmospheric pressure chemical ionisation liquid chromatography/ion trap mass spectrometry. *Rapid Commun. Mass Spectrom.* **2007,** *21,* 880.

[18] H. M. Talbot, M. Rohmer, P. Farrimond. Structural characterisation of unsaturated bacterial hopanoids by atmospheric pressure chemical ionisation liquid chromatography/ion trap mass spectrometry. *Rapid Commun. Mass Spectrom.* **2007,** *21,* 1613.

[19] R. R., Moreau, M. J., Powell, S. F., Osman, B. D Whitaker., W. F. Fett, L Roth. D. J. O'Brien. Analysis of intact hopanoids and other lipids from the bacterium *Zymomonas mobilis* by High-Performance Liquid Chromatography. *Anal. Biochem*. **1995,** *224,* 293.

[20] P. A. Fox, J. F. Carter, P. Farrimond. Analysis of bacteriohopanepolyols in sediment and bacterial extracts by high performance liquid chromatography/atmospheric pressure chemical ionisation mass spectrometry. *Rapid Commun. Mass Spectrom.* **1998,** *12,* 609.

[21] M. Blumenberg, R. Seifert, W. Michaelis. Aerobic methanotrophy in the oxic–anoxic transition zone of the Black Sea water column. *Org. Geochem.* **2007,** *38,* 84.

[22] J. P. Sáenz, S. G. Wakeham S. G., T. I. Eglinton, R. E Summons. New constraints on the provenance of hopanoids in the marine geologic record: bacteriohopanepolyols in marine suboxic and anoxic environments. *Org. Geochem.* **2011,** *42,* 1351.

[23] R. J. Malott, C.-H. Wu, T. D. Lee, T. J. Hird, N. F. Dalleska, J. E. A. Zlosnik, D. K. Newman, D. K. Speert. Fosmidomycin decreases membrane hopanoids and potentiates the effects of colistin on *Burkholderia multivorans* clinical isolates. *Antimicrobial Agents and Chemotherapy* **2014,** *58,* 5211.

[24] G. Isaac, S. McDonald, G Astarita. Lipid separation using UPLC with charged surface hybrid technology. Waters Corporation, Milford, MA. **2000**.

[25] J. H. Cvejic, S. Rosa-Putra, A. El-Beltagy, R. Hattori, T. Hattori, M. Rohmer. Bacterial triterpenoids of the hopane series as biomarkers for the chemotaxonomy of *Burkholderia*, *Pseudomonas* and *Ralstonia* spp. *FEMS Microbiol. Lett.* **2000,** *183,* 295.

[26] C.-H. Wu, L. Kong, M. Bialecka-Fornal, S. Park, A. L. Thompson, G. Kulkarni, S. J. Conway, D. K. Newman. Quantitative hopanoid analysis enables robust pattern detection and comparison between laboratories. *Geobiology* **2015,** 13, 391.

[27] K. A Osborne. Environmental controls on bacteriohopanepolyol signatures in estuarine sediments. PhD Thesis, Newcastle University UK. **2016.**

[28] A. Sherry, K. A. Osborne, F. Sidgwick, N. D. Gray, H. M. Talbot. A temperate river estuary is a sink for methanotrophs adapted to extremes of pH, temperature and salinity. *Env. Microbiol Rep.* **2016,** *8*, 122.

[29] M. P. Cooke, H. M. Talbot, P. Farrimond. Bacterial populations recorded in bacteriohopanepolyol distributions in soils from Northern England. *Org. Geochem.* **2008,** *39*, 1347.

[30] C. L. Spencer-Jones, T. Wagner, B. J. Dinga, E. Schefuβ, P. J. Mann, J. R. Poulsen, R. G. M. Spencer, J. N. Wabakanghanzi, H. M. Talbot. Bacteriohopanepolyols in tropical soils and sediments: sources and trends. *Org. Geochem.* **2015,** *89-90*, 1.

[31] M. Lupascu, J. L. Wadham, E. R. C. Hornibrook, R. D. Pancost. Methanogen Biomarkers in the Discontinuous Permafrost Zone of Stordalen, Sweden. *Permafrost and Periglacial Processes* **2014,** *25*, 221.

[32] J. F. van Winden, H. M. Talbot, N. Kip, G.-J. Reichart, A. Pol, N. P. McNamara, M. S. M. Jetten, H. M. J. Op den Camp, J. S. Sinninghe Damsté. Bacteriohopanepolyol signatures as markers for methanotrophic bacteria in peat moss. *Geochim. Cosmochim. Acta* **2012,** *77*, 52.

[33] S. Neunlist, M. Rohmer. The hopanoids of '*Methylosinus trichosporium*': aminobacteriohopanetriol and aminobacteriohopanetetrol. *J. Gen. Microbiol.* **1985,** *131*, 1363.

[34] M. Rohmer. The biosynthesis of the triterpenoids of the hopane series in the Eubacteria: A mine of new enzyme reactions. *Pure and Applied Chemistry* **1993,** *65*, 1293.

[35] B. E. van Dongen et al., H. M. Talbot, S. Schouten, N. P. Pearson, R. D. Pancost. Well preserved Paleogene and Cretaceous biomarkers from the Kilwa area, Tanzania. *Org. Geochem.* **2006,** *37*, 539.

[36] H. M. Talbot, J. Bischoff, G. N. Inglis, M. E. Collinson, R. D. Pancost. Polyfunctionalised bio- and geohopanoids in the Eocene Cobham Lignite. *Org. Geochem.* **2016,** *96*, 77.

[37] H. M. Talbot, P. Farrimond, P. Schaeffer, R. D. Pancost. Bacteriohopanepolyols in hydrothermal vent biogenic silicates. *Org. Geochem*. **2005,** *36*, 663.

[38] J. S. Sinninghe Damsté, W. I. C. Rijpstra, S. Schouten, J. A. Fuerst, M. S.M. Jetten, M Strous. The occurrence of hopanoids in planctomycetes: implications for the sedimentary biomarker record. *Org. Geochem*. **2004,** *35*, 561.

[39] H. M. Talbot, E. C. McClymont, G. N. Inglis, R. P. Evershed, R. D. Pancost. Peat. *Org. Geochem.* **2016,** *97*, 95.

[40] A. S. Bradley, A. Pearson, J. P. Sáenz, C. J. Marx. Adenosylhopane: the first intermediate in hopanoid side chain biosynthesis. *Org. Geochem*. **2010,** *41*, 1075.

[41] J. Rethemeyer, F. Schubotz, H. M. Talbot, M. P. Cooke, K.-U. Hinrichs, G. Mollenhauer. Distribution of polar membrane lipids in permafrost soils and sediments of a small high Arctic catchment. *Org. Geochem.* **2010,** *41*, 1130.

[42] S. Neunlist, M. Rohmer. Novel hopanoids from the methylotrophic bacteria *Methylococcus capsulatus* and *Methylomonas methanica* – (22*S*)-35-aminobacteriohopane-30,31,32,33,34-pentol and (22*S*)-35-amino-3-β-methylbacteriohopane-30,31,32,33,34-pentol. *Biochem. J.* **1985,** *231*, 635.

[43] P. Simonin, B. Tindall, M. Rohmer, M. Structure elucidation and biosynthesis of 31-methylhopanoids from *Acetobacter europaeus*. *Eur. J. Biochem*. **1994,** *225*, 765.

[44] H. P. Nytoft. Novel side chain methylated and hexacyclic hopanes: identification by synthesis, distribution in a worldwide set of coals and crude oils and use as markers for oxic depositional environments. *Org. Geochem.* **2011,** *42*, 520.

Figure Legends

Figure 1. Ring system and side chains of BHPs discussed in the text and listed in Table 1.

Figure 2. (a) Ion-trap APCI MS^2 spectrum of peractylated BHT (see also [14,15]); (b) UPLC/MS-MS APCI product ion scan of peracetylated BHT; (c and d) UPLC/MS-MS APCI product scans of non-derivatised BHT at 20 eV and 30 eV collision energy (CE) respectively. Major fragmentation pathways are indicated on structures.

Figure 3. (a) Ion-trap APCI MS^2 spectrum of peractylated aminotriol (see also [15]); (b) UPLC/MS-MS APCI product scan of peracetylated aminotriol; (c and d) UPLC/MS-MS APCI product scans of non-derivatised aminotriol at 20 eV and 35 eV collision energy (CE) respectively. Major fragmentation pathways are indicated on structures.

Figure 4. (a) Ion-trap APCI MS^2 spectrum of BHT cyclitol ether (CE) heptaacetate (see also [14,15]); (b) UPLC/MS-MS APCI product scan of peracetylated BHT-CE; (c and d) UPLC/MS-MS APCI product scans of non-derivatised BHT-CE at 20 eV and 30 eV collision energy (CE) respectively. Major fragmentation pathways are indicated on structures.

Figure 5. (a) Ion-trap APCI MS^2 spectrum of triacetylated adenosylhopane (see also [17,29]); (b) UPLC/MS-MS APCI product scans of triacetylated adenosylhopane; (c and d) UPLC/MS-MS APCI product scans of non-derivatised adenosylhopane at 20 eV and 30 eV collision energy (CE) respectively. Major fragmentation pathways are indicated on structures.

Figure 6. Selected UPLC APCI MS-MS MRM chromatograms of non-derivatised BHPs on (a) ACE Excel C18 column and (b) Water BEH C18. MRMs: BHT (**Ia**; *m/z* 529 to *m/z* 191), methylated BHT (**IIa** and **IIa**; *m/z* 543 to *m/z* 205), BHT pseudopentose (**In**; *m/z* 691to *m/z*163), adenosylhopane (**Ie**; *m/z* 662 to *m/z* 136), aminotriol (**Id;** *m/z* 546 to *m/z* 528), aminopentol (**Ij**; *m/z* 578 to *m/z* 560) and BHT-CE (**Ic**; *m/z* 708 to *m/z* 162).

Figure 7. (a) HPLC APCI-MS^n mass chromatograms of adenosylhopane (combined di, tri- and tetraacetates) (*m/z* 746+788+830), methylated adenosylhopane (combined di, tri- and tetraacetates) (*m/z* 760+802+844), adenosylhopane Type-2 diacetate (*m/z* 761), methylated adenosylhopane Type-2 diacetate (*m/z* 775), adenosylhopane Type-3 triacetate (*m/z* 802) and methylated adenosylhopane Type-3 triacetate (*m/z* 816). For explanation of identification of the different, but as yet unknown, terminal groups (g and g') (see [29,41]) **(b)** UPLC APCI MS-MS MRM chromatograms of adenosylhopane (**Ie**; *m/z* 662 to 136), methylated adenosylhopane

(**IIe**; *m/z* 676 to *m/z* 136), adenosylhopane "Type 2" (**If**; *m/z* 677 to *m/z* 151), methylated adenosylhopane "Type 2" (**IIf**; *m/z* 691 to *m/z* 151), adenosylhopane "Type 3" (**If'**; *m/z* 718 to *m/z* 150) and methylated adenosylhopane "Type 3" (**IIf'**; *m/z* 732 to *m/z* 150).

Figure 8. (a) UPLC APCI MS-MS MRM chromatograms from TLE of *Methylococcus capsulatus* Bath showing of aminotetrol (**Ii**; *m/z* 562 to *m/z* 544), 3-methylaminotetrol (**IIIi**; *m/z* 576 to *m/z* 558, aminopentol (**Ij**; *m/z* 578 to *m/z* 560) and 3-methylaminopentol (**IIIj**; *m/z* 592 to *m/z* 574).

Table 1. Commonly occurring BHPs and methylated homologues showing observed and predicted product ions for MRM detection. Base peak ion observed for peracetylated structures are indicated to aid comparison with previous studies.

Name	**Structure**	**n**[a]	**[M+H]+**	**[M+H-H_2O]+**	**[M+H-2(H_2O)]+**	**[M+H-n(H_2O)]+**	**[M+H-n(H_2O)-NH_3]+**	**A+B rings**	**Other ions**	**$TGOH_2^+$**[b]	**TG^+**	**Base peak when acetylated**
			m/z	***m/z***	***m/z***	***m/z***	***m/z***	***m/z***	***m/z***	***m/z***	***m/z***	***m/z***
BHT	**Ia**	4	547	**529**[c]	511	475		191[d]	163[d]			655
Methyl-BHT	**IIa, IIIa**	4	561	**543**	525	489		205	177			669
Pentol	**Ig**	5	563	**545**	527	473		191	163			713
Hexol	**Ih**	5	579	**561**	543	471		191	163			771
Aminotriol	**Id**	3	**546**[c]	528[d]	510	492	475	191	163			714
Methyl-Aminotriol	**IId, IIId**	3	**560**	542	524	506	489	205	177			728
Aminotetrol	**Ii**	4	**562**	544	526	490	473	191	163			772
Methyl-Aminotetrol	**IIIi**	4	**576**	558	540	504	487	205	177			786
Aminopentol	**Ij**	5	**578**	560	542	488	471	191	163			830
Methyl-Aminopentol	**IIIj**	5	**592**	574	556	502	485	205	177			844
BHT Glucosamine	**Ib**	3	**708**	690	672	636		191		180	162[d]	1002
BHT-Cyclitol ether	**Ic**	3	**708**	690	672	636		191	222	180	162	1002
Methyl-BHT Cyclitol ether	**IIc, IIIc**	3	**722**	704	686	650		205		180	162	1016
Bhpentol Cyclitol ether	**Ik**	4	**724**	706	688	652		191		180	162	1060
Methyl-Bhpentol cyclitol ether	**IIk, IIIk**	4	**738**	720	702	666		205		180	162	1074
Bhhexol-cyclitol ether	**Im**	5	**740**	722	704	668		191		180	162	1118
Methyl-Bhhexol cylcitol ether	**IIm, IIIm**	5	**752**	734	716	680		205		180	162	1132
BHT pseudopentose	**In**	3	709	**691**	673	637		191	163	181	163	943
Methyl-BHT pseudopentose	**IIn**	3	723	**705**	687	651		205	177	181	163	957
Adenosylhopane	**Ie**	2	**662**								136[d]	746/788/830[e]
Methyl-Adenosylhopane	**IIe**	2	**676**								136	760/802/844[e]
Adenosylhopane Type 2	**If**	2	**677**								151	761[f]
Methyl-adenosylhopane Type 2	**IIf**	2	**691**								151	775[f]
Adenosylhopane Type 3	**If'**	2	**676**								150	802[g]

Methyl-adenosylhopane Type 3	**IIf'**	2	**690**	150	816[g]

559

560 [a] N indicates number of OH groups in intact structure

561 [b] TG = Terminal Group (at C-35 position; Fig. 1)

562 [c] ions indicated in bold font are base peak ions under positive ion APCI and should be used as parent ions for MRMs

563 [d] ions with single underline are potential product ion targets for MRM transitions

564 [e] di-, tri- and tetraacetate forms are known for these structures[29]

565 [f] diacetate only

566 [g] triacetate only

567

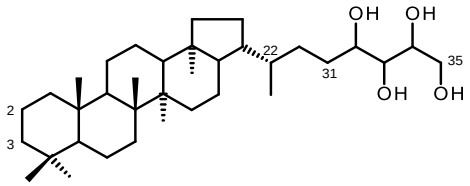

Ia

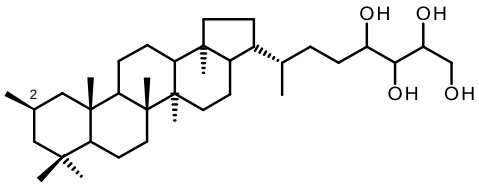

IIa

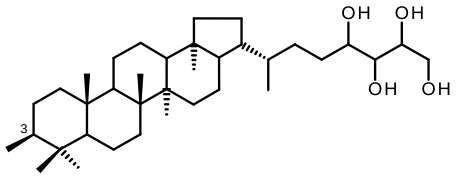

IIIa

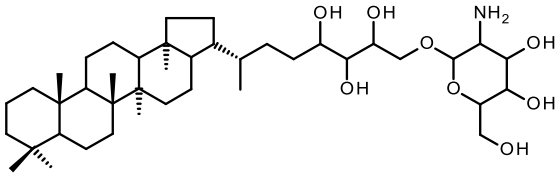

Ib

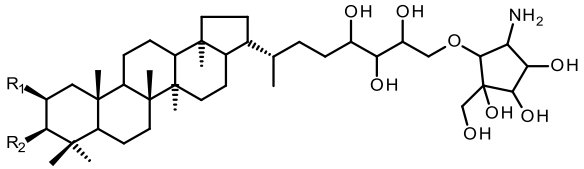

$R_1 = R_2 = H$: **Ic**
$R_1 = CH_3$, $R_2 = H$: **IIc**
$R_1 = H$, $R_2 = CH_3$: **IIIc**

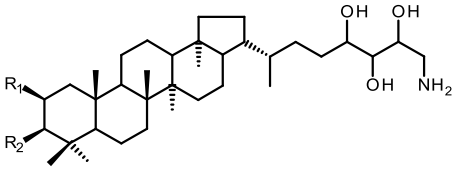

$R_1 = R_2 = H$: **Id**
$R_1 = CH_3$, $R_2 = H$: **IId**
$R_1 = H$, $R_2 = CH_3$: **IIId**

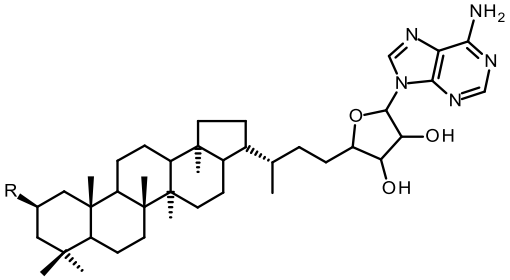

R = H: **Ie**
R = CH_3: **IIe**

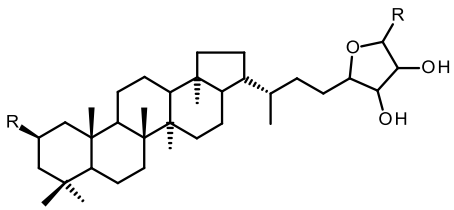

R = H: **If and If' (R = unknown)**
R = CH_3: **If and If' (R = unknown)**

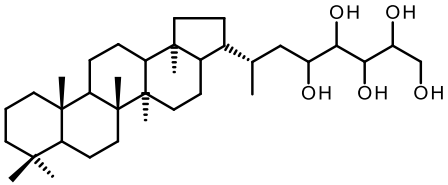

Ig

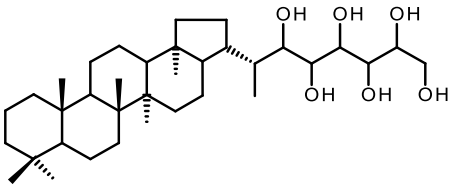

Ih

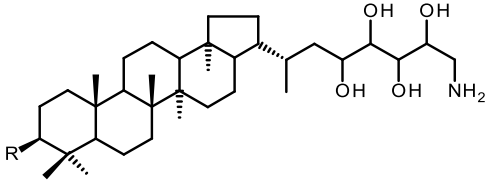

R = H: **Ii**
R = CH_3: **IIIi**

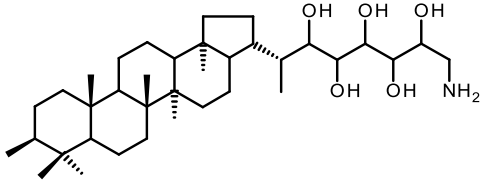

R = H: **Ij**
R = CH_3: **IIIj**

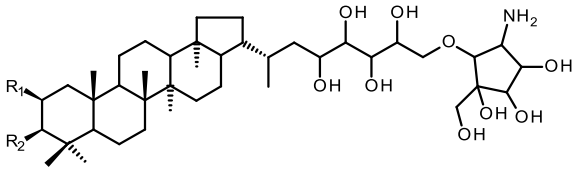

R_1 = R_2 = H: **Ik**
R_1 = CH_3, R_2 = H:**IIk**
R_1 = H, R_2 = CH_3: **IIIk**

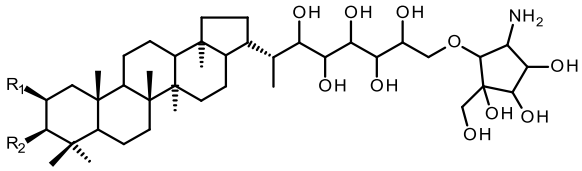

R_1 = R_2 = H: **Im**
R_1 = CH_3, R_2 = H: **IIm**
R_1 = H, R_2 = CH_3: **IIIm**

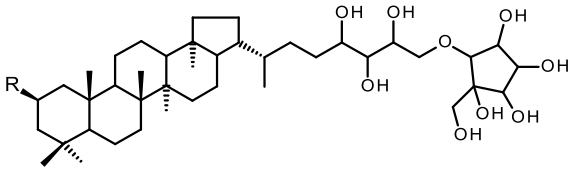

R = H: **In**
R = CH_3: **IIn**

568

569 **Figure 1.** Ring system and side chains of BHPs discussed in the text and listed in Table 1.

570

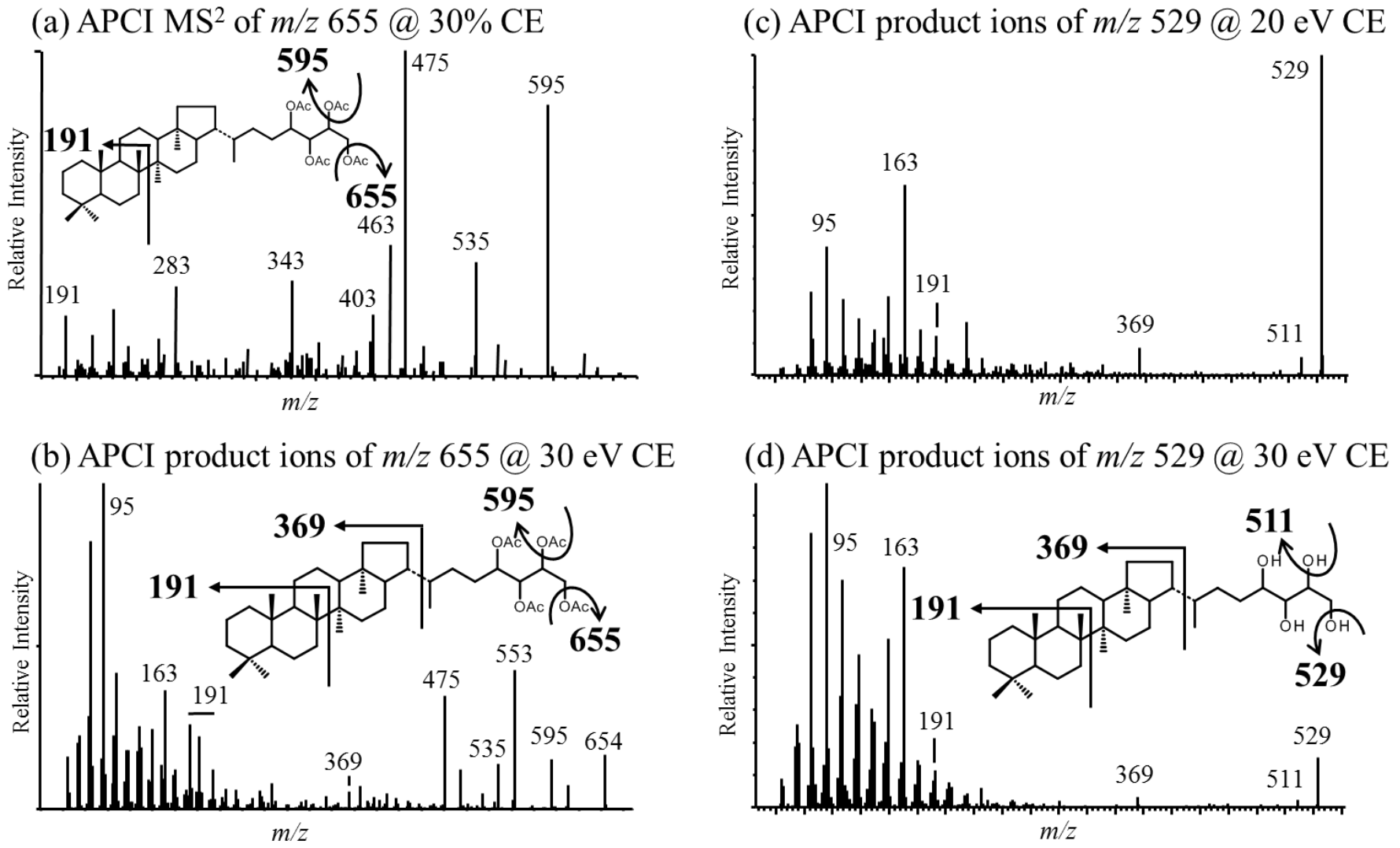
(a) APCI MS² of *m/z* 655 @ 30% CE
595
475
595
191
655
463
535
283
343
191
403
Relative Intensity
m/z
(c) APCI product ions of *m/z* 529 @ 20 eV CE
529
163
95
191
369
511
Relative Intensity
m/z
(b) APCI product ions of *m/z* 655 @ 30 eV CE
95
595
369
191
655
553
163
191
475
535
595
654
369
Relative Intensity
m/z
(d) APCI product ions of *m/z* 529 @ 30 eV CE
511
95
163
369
191
529
191
529
369
511
Relative Intensity
m/z

Figure 2

571

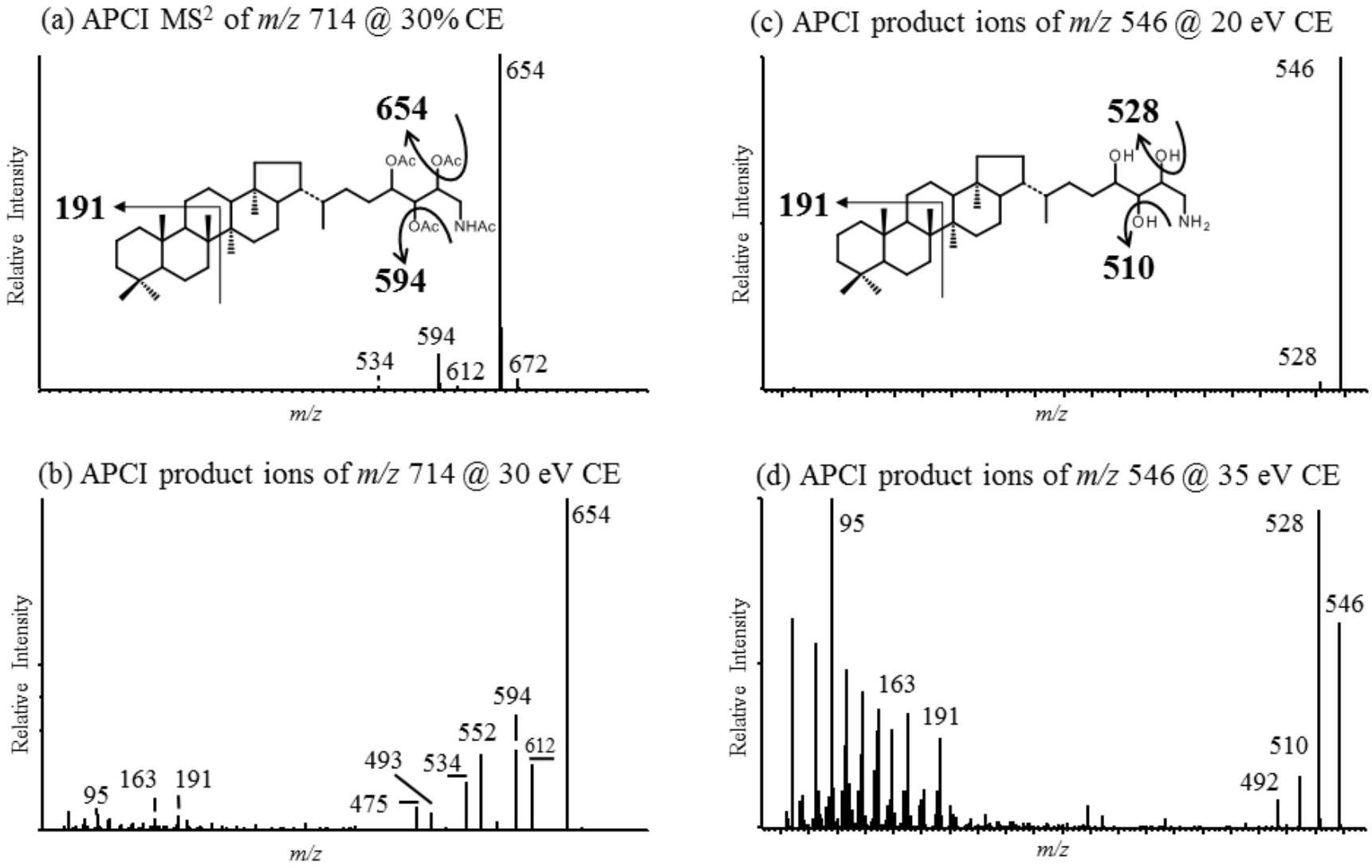
(a) APCI MS² of *m/z* 714 @ 30% CE
654
654
191
OAc
OAc
OAc
NHAc
594
Relative Intensity
594
534
612
672
m/z
(c) APCI product ions of *m/z* 546 @ 20 eV CE
546
528
191
OH
OH
OH
NH₂
510
Relative Intensity
528
m/z
(b) APCI product ions of *m/z* 714 @ 30 eV CE
654
Relative Intensity
594
552
612
493
534
95
163
191
475
m/z
(d) APCI product ions of *m/z* 546 @ 35 eV CE
95
528
546
Relative Intensity
163
191
510
492
m/z

Figure 3

572

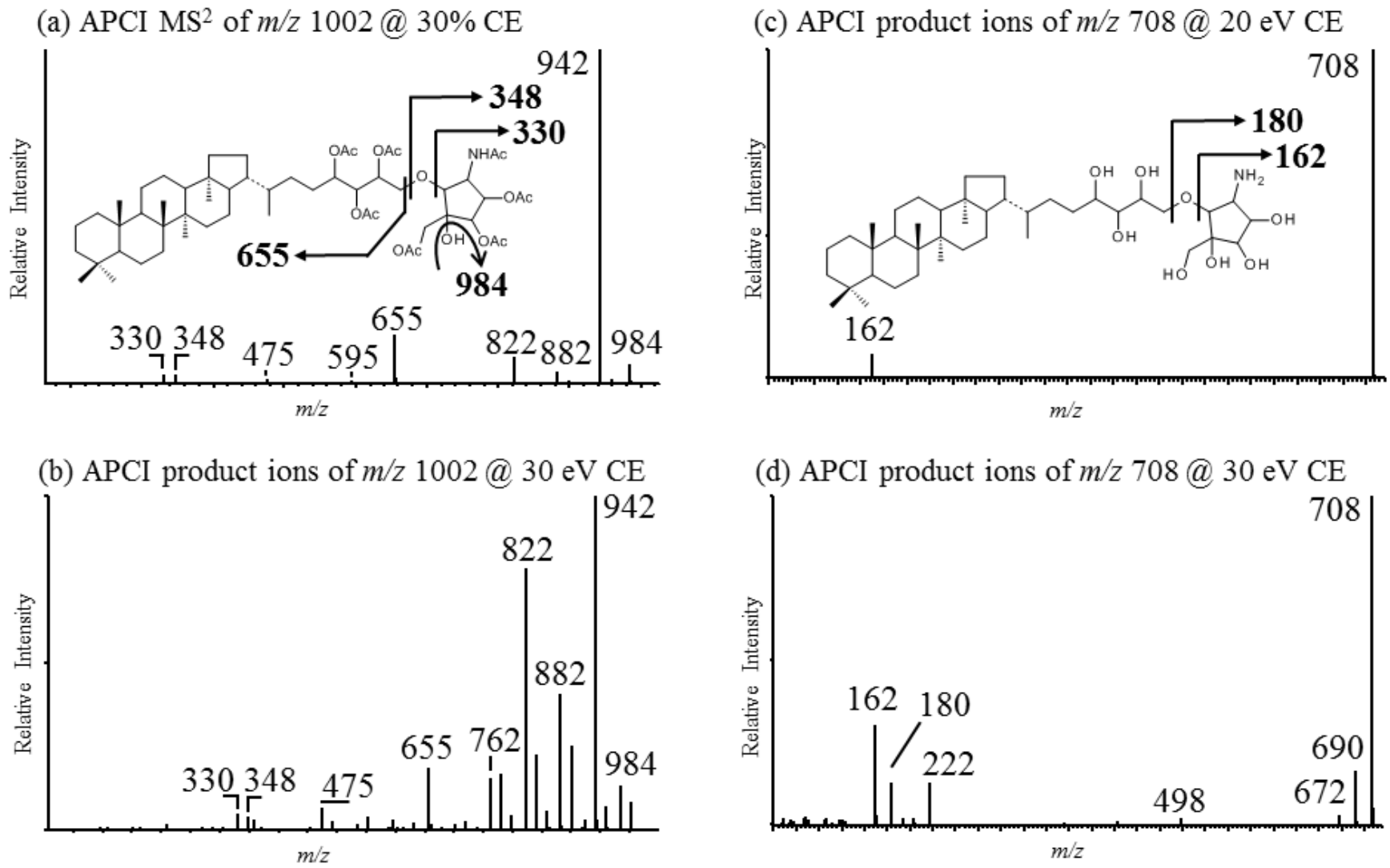
(a) APCI MS² of m/z 1002 @ 30% CE
942
348
330
655
984
330 348 475 595 655 822 882 984
Relative Intensity
m/z
(c) APCI product ions of m/z 708 @ 20 eV CE
708
180
162
162
Relative Intensity
m/z
(b) APCI product ions of m/z 1002 @ 30 eV CE
942
822
882
655 762
984
330 348 475
Relative Intensity
m/z
(d) APCI product ions of m/z 708 @ 30 eV CE
708
162 180
222
498
690
672
Relative Intensity
m/z

Figure 4

573

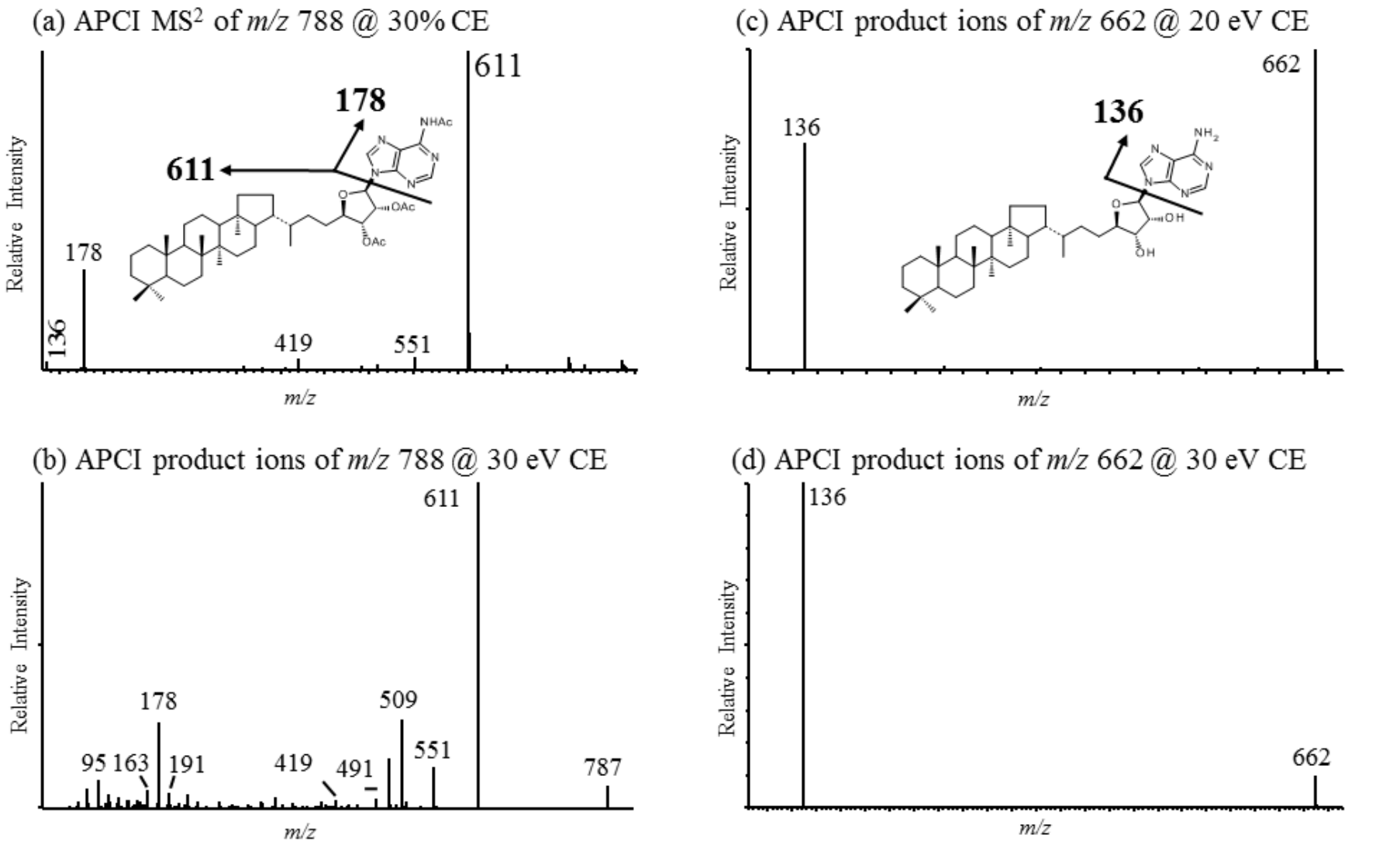
(a) APCI MS² of *m/z* 788 @ 30% CE
611
178
611
NHAc
OAc
OAc
178
136
419
551
Relative Intensity
m/z
(c) APCI product ions of *m/z* 662 @ 20 eV CE
662
136
136
NH₂
OH
OH
Relative Intensity
m/z
(b) APCI product ions of *m/z* 788 @ 30 eV CE
611
178
509
551
95 163
191
419
491
787
Relative Intensity
m/z
(d) APCI product ions of *m/z* 662 @ 30 eV CE
136
662
Relative Intensity
m/z

Figure 5

574

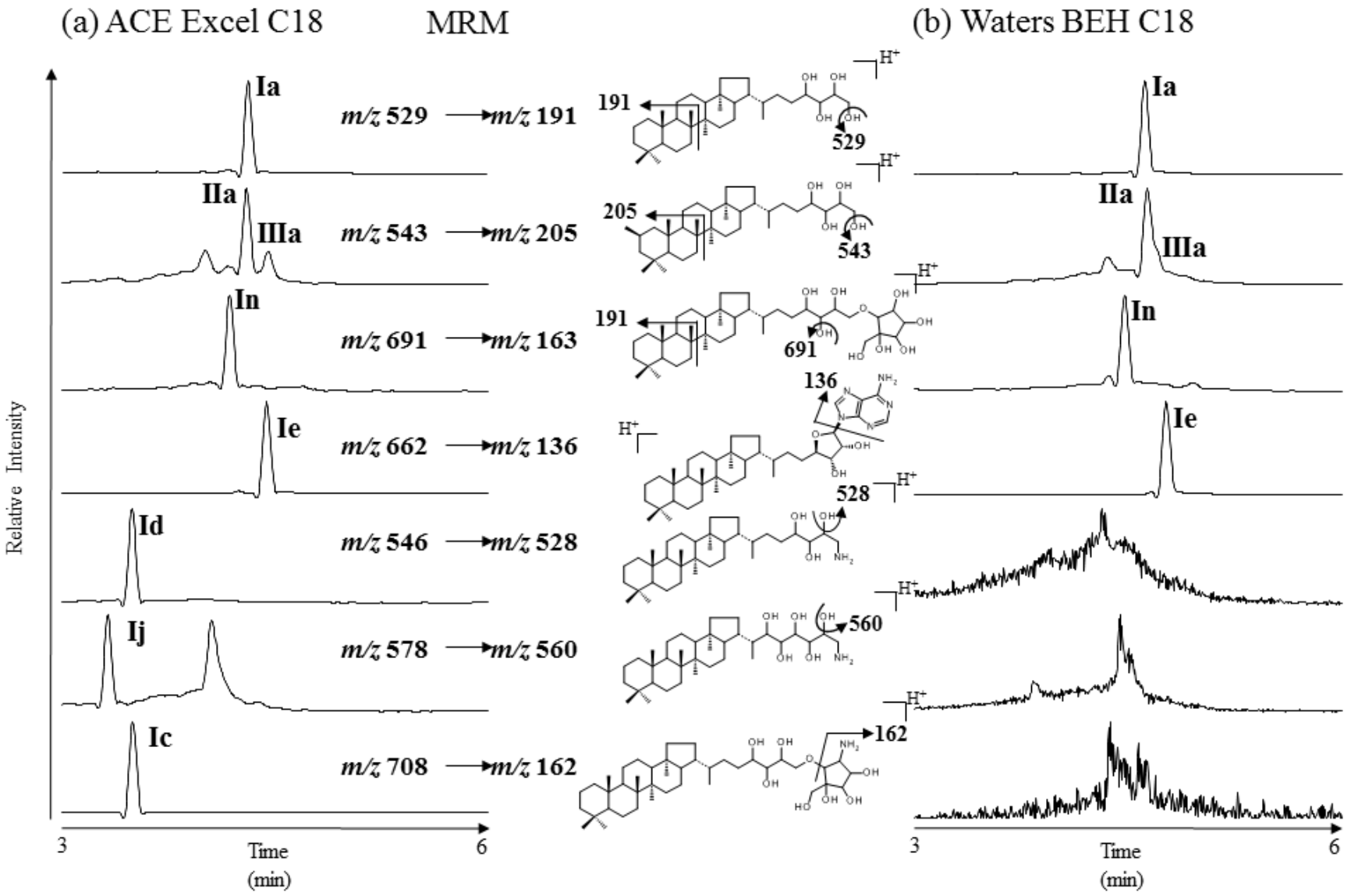

Figure 6[29]

575

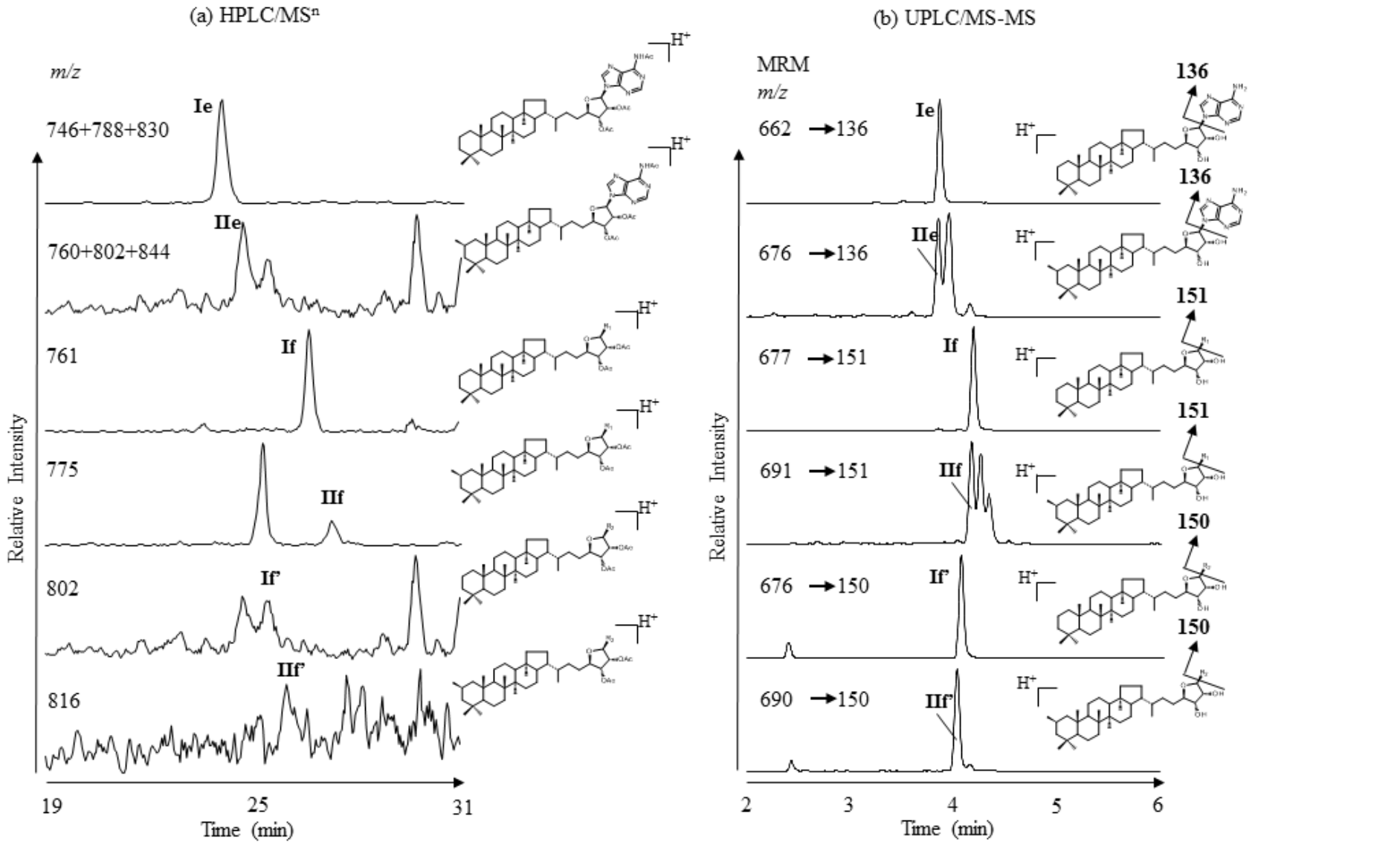
(a) HPLC/MS^n
m/z
746+788+830
Ie
760+802+844
IIe
761
If
775
IIf
802
If'
816
IIf'
Relative Intensity
19
25
31
Time (min)
(b) UPLC/MS-MS
MRM
m/z
662 →136
Ie
676 →136
IIe
677 →151
If
691 →151
IIf
676 →150
If'
690 →150
IIf'
136
151
150
2
3
4
5
6
Time (min)

Figure 7

576

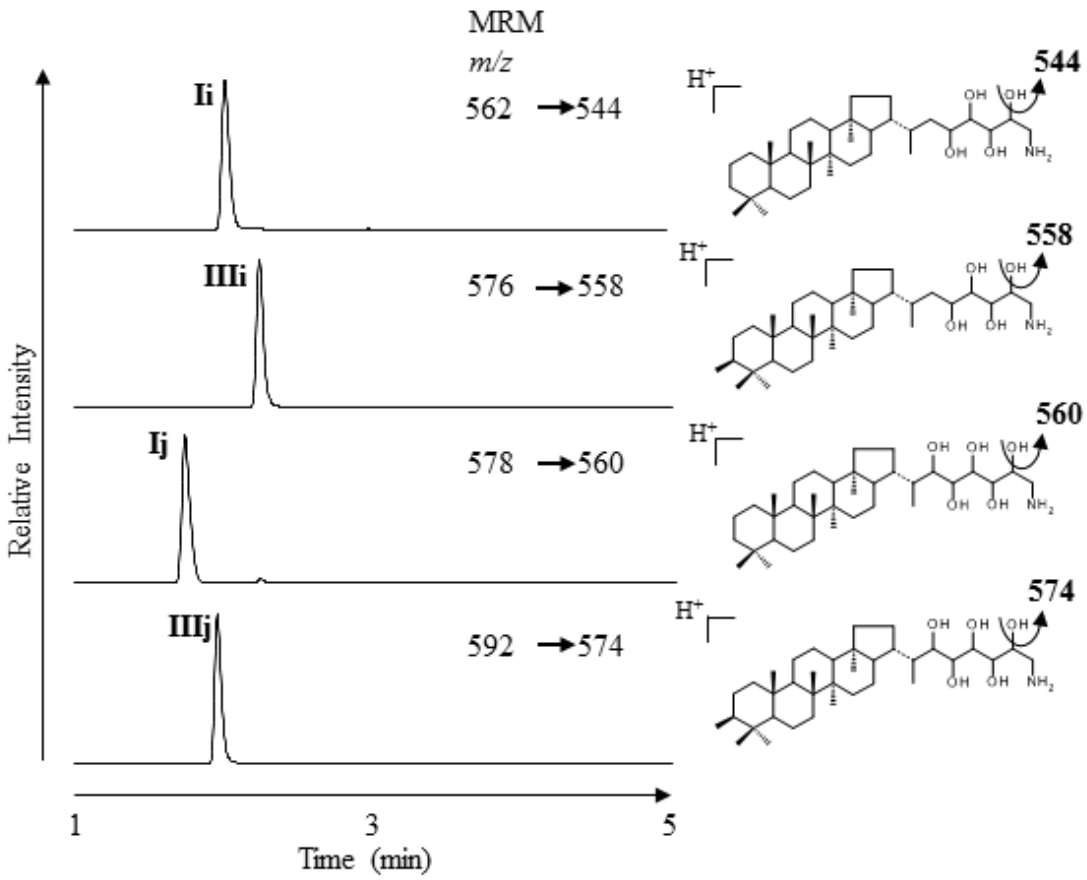
MRM
m/z
Ii
562 →544
544
IIIi
576 →558
558
Ij
578 →560
560
IIIj
592 →574
574
H+
OH
NH2
Relative Intensity
1
3
5
Time (min)

Figure 8

577